THE AMERICAN SOCIETY OF MECHANICAL ENGINEERS
345 E. 47th St., New York, N.Y. 10017

96-GT-146

INVESTIGATION OF WEDGE PROBE WALL PROXIMITY EFFECTS PART1: EXPERIMENTAL STUDY

Peter D. Smout
Rolls-Royce plc.,
Derby, United Kingdom

Paul C. Ivey
School of Mechanical Engineering,
Cranfield University,
Bedford, United Kingdom

ABSTRACT

Conventional 3-hole wedge probes fail to measure the correct static pressure when operating in close proximity to a wall or boundary through which the probe is inserted. The free stream pressure near the outer wall of a turbomachine may be over indicated by upto 20% dynamic head.

This paper reports a series of experiments aimed at quantifying this so-called 'wall proximity effect'. It is shown from a factorial experiment that probe wedge angle, stem design and free-stream Mach number all have a significant influence. The yaw angle sensitivity of wedge probes is also found to depend on the proximity of the probe to the wall of introduction. Flow visualisation studies on large scale probe models are described, and a qualitative model of the probe local flow structures is developed. This model is used to explain the near wall characteristics of the actual size wedge probes. In Part 2 of this paper, the experimental data is used to validate CFD calculations of the flow field around a wedge probe. A simple analytical model of the probe/flow interaction is developed from the CFD solutions.

NOMENCLATURE

B	-	Probe static pressure coeficient $(Sm-p_s)/(p_t-p_s)$
B2	-	B based on S2
B3	-	B based on S3
C_{yaw}	-	Probe yaw angle coefficient $(S2-S3)/(p_t-p_s)$
d	-	Probe stem diameter
I	-	Probe immersion from wall of introduction
I	-	Length of probe interface piece
p	-	Pressure measured in calibration tunnel
S2	-	Pressure indicated by probe left hand static tapping
S3	-	Pressure indicated by probe right hand static tapping
Sm	-	(S2+S3)/2

Suffices

s	-	static value
t	-	Total Value

1. INTRODUCTION

The three hole pneumatic wedge probe (figure 1) is one of several traverse probe designs used commonly for two dimensional flow measurements in turbomachinery. Although less compact than alternatives such as the cobra probe, the wedge probe design is inherently robust, and relatively insensitive to changes in the prevailing flow conditions. Time-resolved pressure measurements in unsteady flows have been made successfully using dynamic wedge probe derivatives with miniature pressure transducers installed in the wedge faces, (Cook, 1988). Bubeck and Wachter (1987) resolved three-dimensional turbomachinery flows using a wedge probe with a fourth pressure tapping installed on an inclined probe tip.

Despite widespread use in unsteady turbomachinery flows, pneumatic pressure probes are steady state devices which indicate an averaged value of the fluctuating pressure. The precise relationship between the probe indicated pressure and the required mean pressure depends on unsteady flow effects around the probe body, and pneumatic averaging in the pipes connecting the probe tappings to remote transducers. Detailed studies have been undertaken by Humm et al. (1994) and others, but the errors associated with measuring unsteady pressures with essentially steady state probes are not fully understood.

Two further sources of error which occur even under steady flow conditions are discussed in the literature. Wedge type probes fail to sense the correct static pressure when operating in close proximity to a wall through which the probe is introduced, yet well outside the boundary layer. This phenomena is termed the 'static pressure wall proximity effect' (Smout, 1990), and is illustrated in figure 2, (Cook, 1988). Cook calibrated three wedge probes having included angles of 23°, 30° and 40° respectively.

Presented at the International Gas Turbine and Aeroengine Congress & Exhibition
Birmingham, UK — June 10-13, 1996
This paper has been accepted for publication in the Transactions of the ASME
Discussion of it will be accepted at ASME Headquarters until September 30, 1996

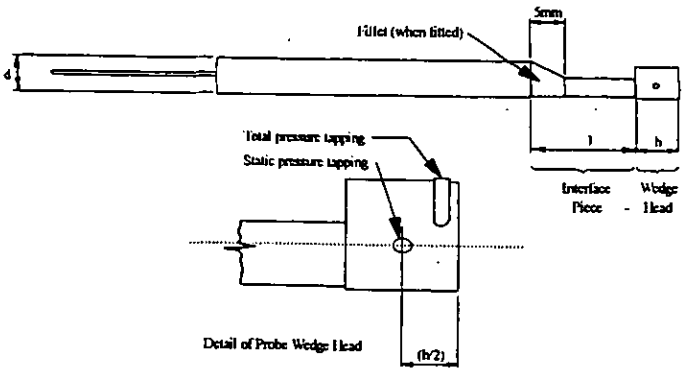

FIGURE 1: Wedge Type Pneumatic Pressure Probe

Each probe was traversed across a 150mm diameter closed section wind tunnel operating at 0.5 Mach number. Figure 2 shows the variation of static pressure coefficient, B, with immersion from the tunnel wall, where B is defined as the difference between the mean probe indicated static pressure and the true static pressure, normalised by the true dynamic head. All the probes indicated a static pressure near to the wall which was higher than that at larger immersions by an amount which increased as the wedge angle increased.

The second error source relates to the type of facility in which a wedge probe is calibrated. Fransson (1983) reports a cross-calibration exercise of the same 46° included angle wedge probe using eleven wind tunnels located throughout Europe. Calibrations at zero incidence over a Mach number range of 0.3 to 1.5 were completed in each facility. In collating the results, Fransson concluded that the probe read a higher static pressure in the free jet than in the closed section type of facility at nominally the same flow condition. From a detailed investigation of pressure probe characteristics, Humm et al.(1994) showed that the apparent sensitivity to yaw angle of a 45° wedge probe was higher in a closed section tunnel than in a free jet.

Part 1 of this paper reports a comprehensive series of experiments aimed at quantifying and understanding the wedge probe wall proximity effect and the calibration facility dependence effect over a wide range of representative test conditions. The results are discussed to arrive at a qualitative explaination of the flow mechanisms responsible for the two effects. In part 2 of this paper, (Smout and Ivey, 1996 (2)), the experimental results are used to validate numerical calculations of the flow around a wedge probe geometry. It is shown that the key flow features can be represented analytically to arrive at a simple model for predicting each effect, given a knowledge of the probe geometry and flow conditions.

2. DESIGN OF INVESTIGATION

The literature showed that the wall proximity effect was influenced by probe shape, by the prevailing flow conditions, and by the way in which the probe was presented to the flow. Because the background information was limited, and because turbomachinery flows are complex, effort was concentrated on establishing the relative importance of variables in a steady flow environment only. Section 3 reports experiments performed with wedge probes typical

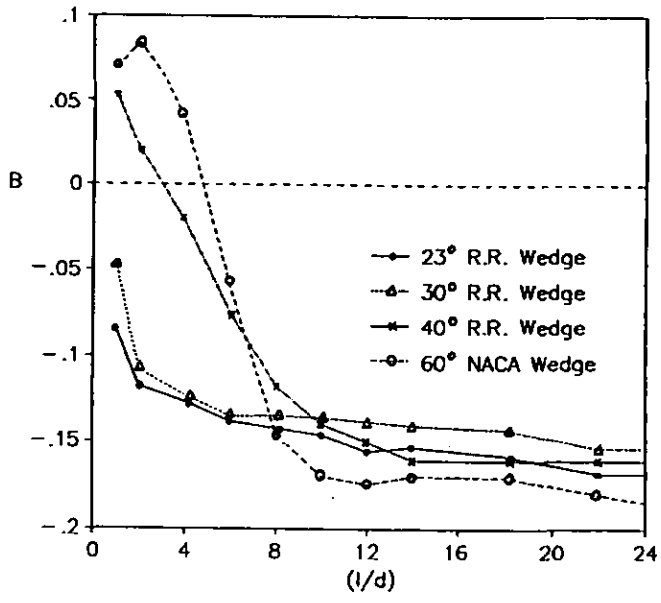

FIGURE 2: Wedge Probe Wall Proximity Effect (Cook, 1988)

of those used for turbomachinery flow measurement. A factorial experiment was designed in which the influence of probe wedge angle, stem length, stem shape, flow yaw and pitch angles on the wall proximity effect were quantified at representative flow Mach numbers and turbulence intensities. This was achieved by traversing wedge probes of 6.35mm diameter in a 200mm diameter, closed section wind tunnel, (section 3.1). A truncated series of traverses was completed with the same probes in a low-speed compressor annulus to determine the influence of casing shape on the wall proximity effect. Section 3.2 describes an experiment to investigate the effect of the wind tunnel wall on probe yaw angle sensitivity. A definitive data set was also required on which to base the investigation of calibration facility dependence. This was estahlished by calibrating four wedge probes in a closed flow and two open jet flows of different size, (section 3.3)

The actual probe experiments were essential in quantifying the two effects, but they were not expected to provide much insight into the physical cause. A series of large scale model tests were arranged for this purpose, and are reported in section 4. Smoke flow visualisation tests were completed with various two-dimensional wedge shapes, and with an eight times scale model of a 30° included angle wedge probe. Pressure measurements at the probe model surfaces were also made. Results are discussed in section 5.

3. ACTUAL PROBE TESTS

3.1 Wind Tunnel Factorial Experiment

A 200mm internal diameter circular section wind tunnel with a bellmouth intake was chosen for the factorial experiment. A centrifugal fan was used to draw air at Mach numbers ranging between 0.1 and 0.8. Free stream turbulence intensity could be increased from 0.8% to 4.5% by introducing a square mesh of

VARIABLE	HIGH VALUE	LOW VALUE
Wedge Angle	60°	24°
Interface Piece Length	20mm	6mm
Fillet	Fitted	Not fitted
Mach Number	0.75	0.35
Turbulence Intensity	4.5%	0.8%
Yaw Angle	+10°	0°
Pitch Angle	-10°	0°

TABLE 1: High and Low Values of Each Variable Used in Factorial Experiment

circular wires at a plane 168mm upstream of the traverse plane. To avoid the adverse influence of strong pressure gradients generated by the turbulence grid near the tunnel walls, a verticle plate was installed at the half radius position to act as the probe wall of introduction. The uniformity of the free-stream static pressure profile at the traverse plane was checked and found to differ from the pressures measured at static tappings in the tunnel walls by less than 1% dynamic head under all tested flow conditions. Further details of the wind tunnel and of the flow characterisation exercise were given by Smout and Ivey (1994).

High and low values of each variable to be used in the factorial experiment were chosen to bracket those typically encountered in turbomachinery rig testing. For example, an included wedge head angle of 24° is the smallest that can realistically be achieved, whilst 60° is the largest angle that is normally used to avoid excessive blockage. Table 1 summarises the high and low values chosen for each variable. Traverses were completed with every combination of high and low values, experiments being conducted in random order to reduce the risk of systematic error.

The results from each experiment were plotted as static pressure coefficient vs. normalised probe immersion to give curves which qualitatively resembled the curves in figure 2. The area under the curve was computed in each case, and used to indicate the severity of the wall proximity effect in terms of the deviation of static pressure coefficient from the 'free-stream' value, and the immersion over which this deviation occured. Further data reduction was performed using the 'Yates' technique (Davies, 1978) for comparing the results of a suitable number of factorial experiments in a sequential manner to quantify the relative effect of each variable, and interactions between variables. Each effect and interaction was tested against criteria based on the uncertainties associated with the experiment to determine its significance.

In brief, it was found that the length, l, of the interface piece had a strong influence on the wall proximity effect, where moving the wedge head away from the circular stem by increasing 'l' gave a marked reduction in wall proximity effect. This is illustrated in figure 3, where the wall proximity curves for 24° probes with long and short interface piece lengths are overlayed. All other conditions between these two experiments were identical. A difference in static pressure coefficient (B) values for the two probes was also observed (see figure 3), where increasing the interface piece length from 6mm to 20mm raised B from -0.16 to -0.07 respectively. Three further variables of significance were wedge head included angle, Mach

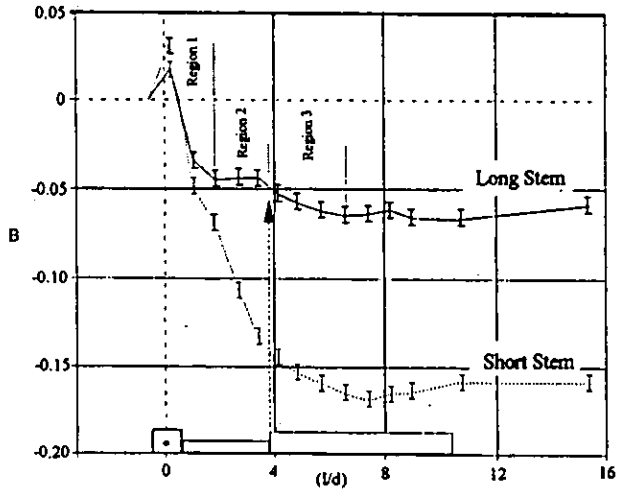

FIGURE 3: Influence of Interface Piece Length on Wall Proximity Effect

number and pitch angle, where an increase in any one variable accentuated the wall proximity effect. Less significant were the effects of a stem fillet and the free stream turbulence intensity, and probe yaw angle had no detectable effect. A fuller discussion of the results from this experiment is given by Smout and Ivey (1994).

To check that the wall proximity effect was independent of the precise geometry of flow ducting, the 24° wedge probes were traversed radially at the I.G.V. inlet plane of the Cranfield University low speed, four-stage compressor rig, (Howard et al., 1993). The compressor rig results agreed with the wind tunnel results to within the limits of experimental uncertainty for all tested conditions.

3.2 Near Wall Yaw Angle Calibrations

The effect of yaw angle on the wall proximity effect was shown from the factorial experiment to be insignificant, but it was observed by Morris (1961) that wedge probe yaw angle *sensitivity* could be influenced by the close proximity of a wall. Yaw sensitivity is the per degree change in yaw coefficient, C_{yaw}, where C_{yaw} is defined as the difference between the probe static tapping readings, normalised by the true dynamic head. The influence of the wall on yaw angle sensitivity was investigated by calibrating wedge probes against yaw angle at four probe immersions. In general, C_{yaw} was directly proportional to yaw angle over ±8° of yaw, beyond which the change in C_{yaw} was non-linear but still monotonic with yaw angle increasing up to at least ±20° of yaw. A marked difference between the four calibrations was apparent outside the linear region.

The slope of the linear region between ±8° yaw, (i.e. the probe yaw sensitivity), is plotted against immersion in figure 4, where yaw sensitivity is seen to increase by 12% between 15mm and 60mm immersion. Also plotted in figure 4 is the wall proximity effect curve for the same probe; yaw angle sensitivity is apparently affected over a similar immersion range to static pressure. Assuming that the calibration value at 60mm were applied in analysing radial traverse data from a turbomachine, at 0.1 Mach number and a probe setting angle of 5° relative to the flow, a near wall measurement error of +0.7° would result from this yaw-angle wall proximity effect.

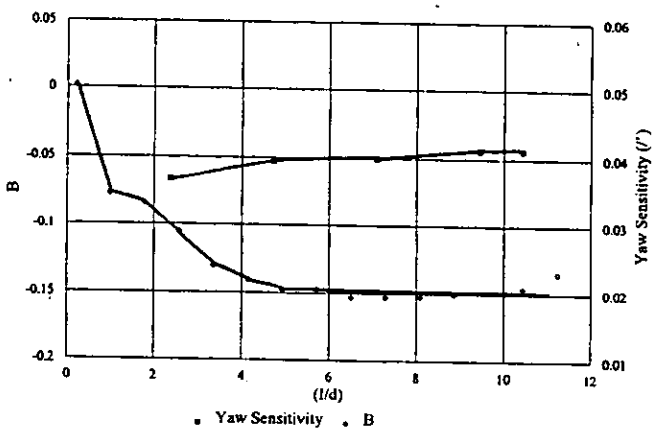

FIGURE 4: 30° Wedge Probe Calibration Against Immersion at 0.1Mn

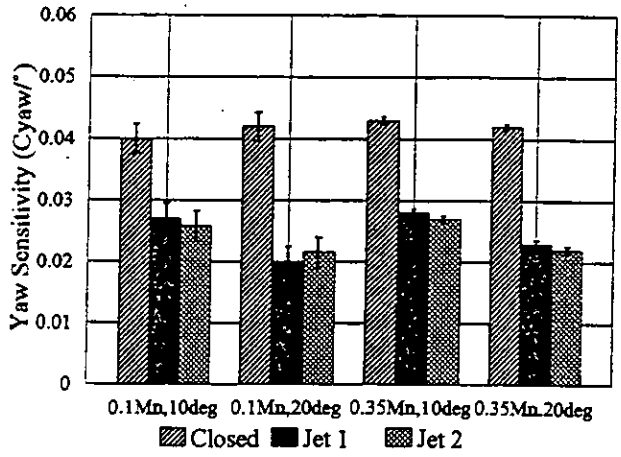

FIGURE 5: Comparison Between Yaw Sensitivities of Short, 24° Probe in Open and Closed Flows

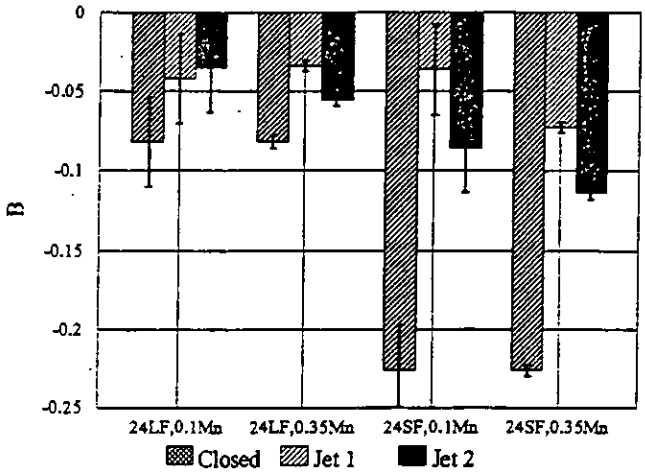

FIGURE 6: Comparison Between B Values for 24° Probes in Open and Closed Flows

3.3 Calibration Facility Dependence

From the literature, it was known that calibrations of static pressure coefficient vs. Mach number for a given wedge probe depended on whether a closed duct or a free jet calibration flow were used, (Fransson, 1983), and also possibly on the free jet diameter, (Shreeve, 1976). No information on the influence of probe geometry or incidence angle could be found. An experiment was designed in which the four wedge probes used in the factorial experiment (section 3.1) were calibrated in two open jets of different cross-sectional area, and in the closed section wind tunnel described in section 3.1. The general arrangement of the two open jet facilities was similar, the smaller facility (Jet 1) having a 50mm by 30mm rectangular section nozzle, and the larger facility (Jet 2) an octagonal section nozzle 102mm across flats. Both flows were characterised to ensure uniformity of static pressure at the traverse plane.

Individual calibrations of each probe were completed in each facility at Mach numbers of 0.10 and 0.35. Probes were positioned in the open jets such that the plane of static tappings lay on the jet centre line, and at 100mm immersion in the closed wind tunnel to avoid wall proximity effects. Yaw angle sensitivities were derived for each probe from the C_{yaw} characteristics, for yaw angle ranges of 0° to 10° and 0° to 20°. Values obtained at each Mach number and in the three facilities were grouped together under probe type and plotted in bar chart form, as shown in figure 5 for the short interface piece 24° probe. Static pressure coefficient values at zero yaw were grouped as a function of the probe included wedge angle; a bar chart summary of the 24° probe data is given in figure 6. For both yaw sensitivity and static pressure coefficient, substantial differences particularly between the closed tunnel and open jet, but also between the two open jet calibrations were observed.

4. MODEL PROBE TESTS

4.1 Two Dimensional Models

The flow over various large scale, two dimensional wedge shapes was studied in a smoke flow visualisation tunnel at the Cranfield University College of Aeronautics. This tunnel conforms with the general guidelines for smoke flow tunnel design given by Mueller (1983); flow is accelerated from the inlet settling chamber through a two dimensional contraction of 8:1 into the working section, and a multi-point smoke rake mounted vertically in the contraction can be moved radially and laterally to align smoke filaments with features of interest on the model. Stable, dense smoke filaments can be sustained at velocities between 2 and 10m/s.

Wedges with included angles of 24° and 60° were constructed to simulate the actual probes tested in the factorial design experiment. A x30 scaling factor was used to give turbomachinery representative Reynolds numbers (based on wedge chord) of upto 11×10^4, although representative Mach numbers could not be reproduced due to the velocity limit imposed by the smoke flow technique. The wedge leading edges were made detachable at a transverse line 10% chord back from the wedge apex, such that rounded leading edges could be substituted. Wedges were mounted in turn on to a disc in the tunnel back wall, and rotated to present the model at any required angle to the flow. Smoke flow patterns were recorded using video and still photography.

Figure 7 shows the flow around the sharp nosed 24° wedge model inclined at 8° to the flow, at a Reynolds number of

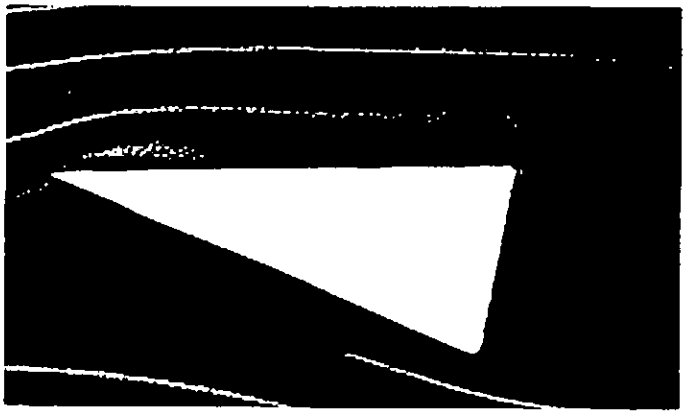

FIGURE 7: Visualisation of Flow Over 2-D 24° Wedge Model at 8° Yaw and $5.2x10^4$ Re

$5.2x10^4$. Well defined, laminar smoke filaments were observed in the free stream flow away from the model, and near the model pressure surface. Although some detail of the suction surface flow was obscured by shadow, the flow lifted noticeably immediately downstream of the leading edge before moving back towards the wedge face further downstream. Diffusion of the same suction surface smoke filament just downstream of the leading edge was apparent from the corresponding video film, indicative of a suction surface separation bubble in the leading edge region at yaw angles of 8° and above.

As the yaw angle of the 24° probe was increased beyond 8°, the reattachment point moved progressively further back along the wedge suction surface until complete separation without re-attachment occurred at 20° yaw. A stagnation point was observed on the pressure surface, just downstream of the leading edge, about which the flow divided. This stagnation point migrated away from the leading edge as yaw angle was increased. Generally similar results were recorded for the 60° wedge model, with suction surface flow separation beginning at 18° yaw, followed by complete separation without re-attachment at 30° yaw. Radiusing the leading edge of the 24° wedge made little observable difference over the whole yaw angle range, but the suction surface separation bubble on the blunt nosed wedge formed at a lower yaw angle of 4°. Fitting a rounded leading edge to the 60° wedge had more effect, and delayed the onset of transition and complete separation without re-attachment to higher yaw angles. As with the 24° wedge, suction surface separation was evident in the blunt nosed 60° model at 4° yaw. Although variations in the size and structure of the separation bubble might have been expected as a function of Reynolds number, the suction surface flow was not visualised in sufficient detail to detect any such changes.

4.2 Three Dimensional Models

A 0.61m square section wind tunnel at Sheffield University was used for smoke flow visualisation experiments on a x8 scale model of a 30° wedge probe. The wind tunnel was similar to the Cranfield tunnel in layout, but with an 18:1 three-dimensional contraction from the inlet to the working section. Optical access was available from each side and through the tunnel roof at the working section. A flat plate was installed 100mm in from one verticle wall to replicate the environment in which the actual probe factorial experiments were conducted. The static pressure profile at the traverse plane was found to vary by less than ±1.5% dynamic head at all flow conditions.

The choice of a x8 scaling factor for the model probe gave a traverse distance from wall to wall of ten probe stem diameters, sufficient to cover the extent of static pressure wall proximity effects observed in the factorial experiment. The model was fabricated in stainless steel with static pressure tappings incorporated at various locations over the wedge faces and in the stem leading and trailing edge regions, (see figures 8 and 9). These were intended for mapping the probe surface static pressure distribution as a function of probe immersion, yaw angle and flow condition.

4.2.1 Pressure Measurements

To establish whether this low speed experiment was representative of the actual scale probe factorial experiment, a series of large scale probe traverses were conducted at 0° yaw, and at Reynolds numbers between $1.7x10^4$ and $11.3x10^4$. Water manometers were used to measure the pressure at each probe surface pressure tapping simultaneously. As in the factorial experiment, the tunnel speed was adjusted at each immersion to retain a constant dynamic head throughout the traverse, thus compensating for probe blockage effects. Calibrations against yaw angle were conducted at an immersion of eight times the probe stem diameter to avoid wall proximity effects.

In figure 8, B for six of the wedge face static tappings is plotted against the normalised probe immersion (I/d), for a Reynolds number of $8.3x10^4$. The probe is drawn to scale against the absisca of this plot such that the correspondence between a set of data points and the probe position relative to the flat plate can be visualised. (For example, at 2d immersion, the probe wedge head and half of the interface piece were immersed in the flow, etc.). Tapping no.4 is the closest in position to the static tappings of the actual probes used in the factorial experiment; this tapping indicates a fall in static pressure with increasing immersion which is characteristic of the wall proximity effect, and of a similar magnitude. Like behaviour is observed with the other tappings, the magnitude of change in B depending primarily on the distance back from the leading-edge, and to a lesser extent on the stemwise displacement of the tapping from the probe tip. A discontinuity in the curves for tappings 3 and 6 at three stem diameters immersion is observed, and corresponds with the emergence of the circular probe stem into the flow. The variation of static pressure at the back of the probe as a function of probe immersion at a Reynolds number of $8.3x10^4$ is plotted in figure 9. The beginning of each curve corresponds with the emergence of each successive pressure tapping.

In figure 10, B values for six of the wedge face static pressure tappings are plotted against yaw angle. The curves bunch together in three groups at positive incidence, the lower group comprising the curves for the two rear most tappings, (3 and 6), and the upper group the curves for the two near-most leading edge tappings, (5 and 8). This grouping is lost at negative incidence where the instrumented wedge face becomes the wedge suction surface, and the variation of B with yaw angle is no longer monotonic. It can be infered from figure 10 that probe sensitivity to yaw angle increases as the static pressure tappings are moved

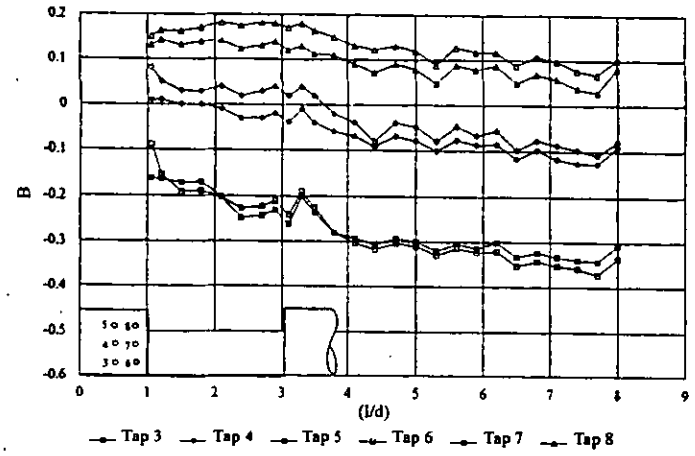

FIGURE 8: Large Scale Wedge Probe Radial Traverse at 25m/s, (taps 3 to 8)

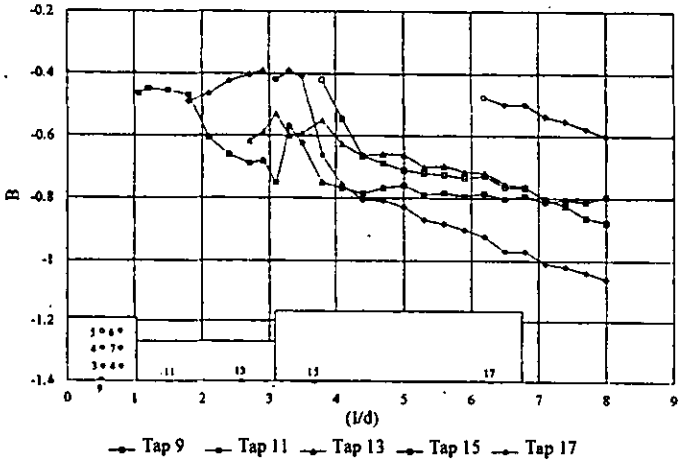

FIGURE 9: Large Scale Wedge Probe Radial Traverse at 25m/s, (taps 9 to 17)

towards the wedge leading edge, as previously shown by Ferguson (1967) and others. Broadly similar calibrations and traverse results were recorded at the other flow conditions.

4.2.2 Smoke Flow Visualisation

The large scale probe was set to the required immersion at a given flow condition, and a single point smoke wand traversed upstream and in the plane of the probe. Good quality flow patterns were recorded onto video at Reynolds numbers of upto 2.0×10^4, but flow features, particularly in the probe wake, became less well defined at higher Reynolds numbers.

Key features of the visualised flow patterns are sketched in figure 11. At 2d immersion, a re-circulation at the up-stream lip of the probe hole of introduction, and a second, stable re-circulatory region at the probe tip, in the wake of the wedge head and in the plane of the probe were observed. It was noted that the size of this second re-circulation increased as the probe was traversed out from the wall, before attaining a stable size at approximately 2d immersion. Faint traces of smoke in the wake of the interface piece suggested flow out of the bottom of the wedge tip re-circulation and down the back of the probe towards the wall. The tip re-circulation could be visualised by aligning the smoke probe with either the top

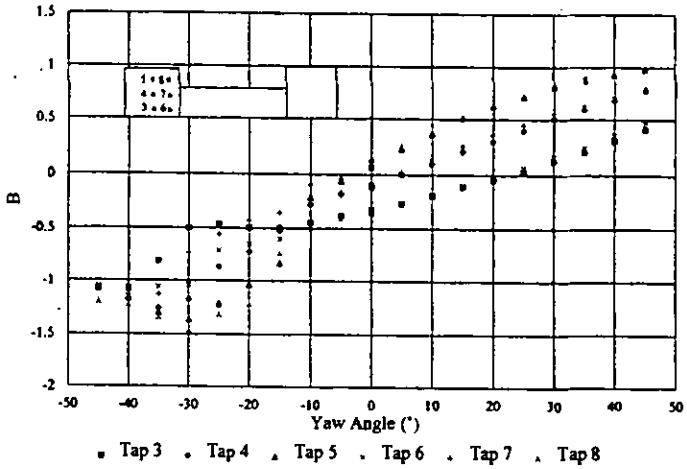

FIGURE 10: Large Scale Wedge Probe Calibration Against Yaw Angle at 25m/s

or bottom end of the wedge head, indicating that flow was sucked in to the wedge wake region from both the free and supported ends.

By 4d immersion, whilst the wedge head wake re-circulation remained at its equilibrium diameter, a re-circulatory flow structure at the base of the cylindrical stem and in the plane of the probe had also formed, and the stemwise flow along the back of the probe had intensified. As the probe immersion was increased further, the re-circulation in the wake of the cylinder continued to grow until stabilising at a constant diameter of approximately 4d at 7d immersion. Beyond this immersion, the structure of the re-circulatory regions in the wake of the wedge head and the cylindrical stem showed little change, but remained locked to the probe with a continual transfer of fluid from the former to the latter along the back of the interface piece.

Flow over the central part of the wedge head was visualised in a plane perpendicular to the probe as the probe yaw angle was varied. At 0^a yaw angle, a pair of contra-rotating vortices were observed in the wake of the wedge head which extended downstream from the base of the wedge by approximately 0.75 wedge chord. As yaw angle was increased, the wake flow became more obviously three-dimensional, with flow from the wedge pressure surface spiralling over the top of that leaving the suction surface. This observation agreed qualitatively with the two-dimensional wedge model flow visualisation experiments. Smoke particles were also observed passing over the tip of the probe from pressure surface to suction surface, but the video image was not sufficiently well resolved to confirm the formation of a separation bubble in the leading edge region of the wedge suction surface at yaw angles greater than 8°, as noted in the two-dimensional model studies.

5. DISCUSSION

Considering first the flow visualisation results, the coherent, stable re-circulatory region identified in the probe wake gives a link between probe immersion and the probe's characteristics. The re-circulation is the result of viscous deceleration of fast moving fluid just downstream of the probe tip, and causes a stemwise velocity component immediately adjacent to the wedge rear face, and towards the probe free end. An associated

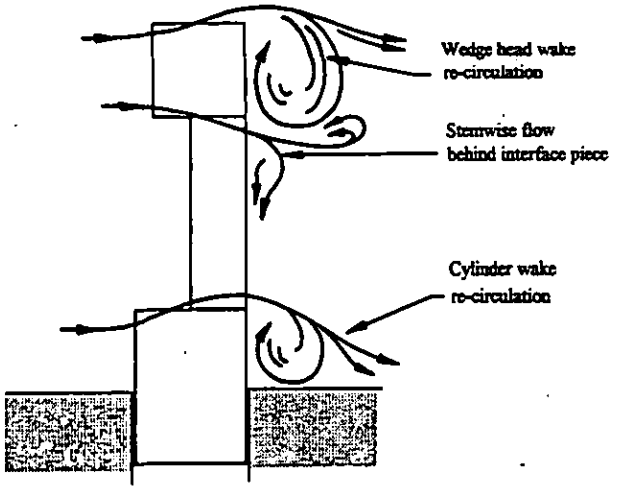

FIGURE 11: Sketch of 3-D Flow Vis. Results: Probe at 4d Immersion

pressure drop is to be expected, of a magnitude depending on the size and structure of the re-circulation and hence on the probe immersion. From figure 9, the fall in static pressure at the back of the wedge indicated by tapping no.9 is 25% dynamic head for immersions between 1d and 3d. By conservation of energy, this reduced base pressure must be accompanied by flow acceleration over the wedge faces, resulting in a reduced pressure at the wedge face static pressure tappings consistent with the wall proximity effect.

Close inspection of the wall proximity curve for the long interface piece, actual size probe (figure 3), shows that B falls through the immersion range defined as region 1 in a manner consistent with the model above. The equilibrium state reached in region 2 indicates that the wedge head is now sufficiently immersed to be free from any influence of the eddy at the hole of introduction, and that the re-circulation in the wedge head wake has attained an equilibrium diameter with a constant associated wedge base pressure. This is consistent with the flow visualisation results in section 4.

The equilibrium state is upset at the beginning of region 3, which corresponds with the emergence of the circular stem through the wall. It is proposed that the re-circulating region established in the wake of the cylinder causes a reduction in the static pressure in this region below that which would be expected for an infinitely long (two-dimensional) cylindrical element. This proposition is suggested by the flow visualisation study results, and supported by experimental data in figure 9, where tappings 15 and 17 positioned in the cylinder trailing edge both indicate a monotonically decreasing pressure with increasing immersion. For this to cause the reduction in indicated static pressure observed through region 3 implies some interaction between the two re-circulating regions. An interaction was apparent in the flow visualisation studies, where stemwise flow down the back of the probe from the wedge re-circulation towards the base of the cylinder was observed. The result is to modify the wedge head wake re-circulation and further increase the momentum of fluid near the wedge faces so reducing the wedge face static pressure further. In the flow visualisation studies, the cylinder wake re-circulation reached an equilibrium diameter at a given immersion beyond which no further growth occurred. This is consistent with the second plateau in the wall proximity curve at the end of region 3 in figure 3.

Developing this argument, a reduction in the length of the interface piece effectively moves the re-circulations behind the wedge and the cylinder closer together. This intensifies the stemwise static pressure gradient, and modifies the wedge wake re-circulation which in turn governs the flow over the wedge faces. A greater wall proximity effect might be expected, and was observed experimentally (figure 3). It follows that the different static pressure coefficients associated with the long and short interface piece probes are determined by the relative strengths of these re-circulations. Much wedge probe research has been conducted by previous investigators using two-dimensional wedge shapes to determine characteristics which are then assumed to hold for three-dimensional probes, (Ferguson (1967) for example). The validity of this approach must be in doubt, since the re-circulations are not established with two-dimensional shapes. If the re-circulating regions were influenced by highly turbulent or periodically unsteady flow typical of turbomachinery, it also follows that the static pressure coefficient would alter from that determined in a steady calibration flow.

This previously un-reported idea of probe characteristics being governed by interacting regions of re-circulating flow in the probe wake is useful in explaining other results from the factorial experiment in section 3.1. For example, changing the pitch angle from 0° to -10° resulted in a significant increase in wall proximity effect which is consistent with the probe wake re-circulation model. Introducing negative pitch effectively reduces the separation between the two discrete re-circulations, and is analogous to reducing the interface piece length. Inclining the probe also axially displaces the two re-circulations relative to each other, which may again influence the interaction between them. Increasing free stream Mach number also resulted in a significant increase in wall proximity effect. It is well known that the pressure drag coefficient for two-dimensional wedge shapes and cylinders increases with increasing Mach number. Because the wall proximity effect depends directly on the wedge base pressure, and indirectly on the pressure at the back of the cylindrical stem, a more severe wall proximity effect is to be expected at higher Mach numbers.

The model is also of use in understanding results from the facility dependence experiments in section 3.2. Figure 6 shows that the static pressure coefficients at zero yaw obtained in the closed tunnel were always lower, (more negative), than the values obtained in the free jet facilities, by up to 18% dynamic head in the worst case. From the flow visualisation studies, it is estimated that the two probe wake re-circulations span a stemwise distance from the probe tip of 51mm for the long interface piece probe, and 37mm for the short interface piece probe. Comparing these values with the jet dimensions, the re-circulation in the cylindrical stem wake would have been influenced by the interface between the free jet and the surrounding stationary air for both probes calibrated in the smaller jet 1, and for the longer probe in jet 2. Assuming that turbulent flow at the free jet boundary dissipates the re-circulating motion behind the cylinder, the probe wake re-ciculation model predicts a higher value of probe indicated static pressure than that in a larger diameter jet flow where both re-circulations were fully developed. This was the case for both the 24° and 60° included angle wedge probes.

Extending the probe wake re-circulation model to explain the various wedge probe yaw characteristics reported in sections 3.2 and 3.3 is difficult, given the limited flow visualisation data at other than 0° yaw. Three ways in which the model could be altered to explain these results are offered, but further work is required in this area.

i) The re-circulating region in the wake of the wedge head may be sucked into the suction surface region of the wake flow when the probe is operated at incidence, and generate a pressure gradient at the base of the wedge with a minimum at the suction surface corner. As immersion is increased, so the re-circulation grows, reducing the base pressure differentially so as to accelerate the flow more rapidly over the suction surface than the pressure surface.

ii) Flow migration over the free end of the wedge head from pressure to suction surface was observed during the flow visualisation studies. Over tip leakage flow may roll up into a tip vortex with its origin at the suction surface trailing edge. The axial velocity associated with such a vortex may locally amplify the re-circulation in the suction surface region of the wedge wake and preferentially accelerate the suction surface flow as before.

iii) It was shown from the two-dimensional wedge flow visualisation studies, (section 4.1), that a separation bubble forms in the leading edge region of the wedge suction surface at yaw angles of 8° and above, and that the re-attachment point moves downstream with increasing yaw angle. Points i) and ii) above imply alterations to the suction surface flow which may influence the formation and growth of the separation bubble, and change the static pressure profiles over the wedge faces in consequence.

Each of points i to iii) link probe yaw measurement characteristics to the probe wake re-circulations. For this link to be valid, yaw sensitivity must be influenced under similar circumstances to probe indicated ststic pressure. In section 3.2 it was shown that the 'yaw angle wall proximity effect' occured over a similar immersion range to the static pressure wall proximity effect, (figure 4). Considering the calibration facility dependence of yaw angle sensitivity reported in section 3.3, values obtained from the two free jet facilities agreed with each other within the limits of experimental uncertainty, but were substantially lower than values obtained in the closed tunnel. Hence, although the flow structures local to a yawed probe have not been fully resolved, there is strong experimental evidence to link the yaw angle measurement characteristics of a wedge probe to the re-circulations which occur in the probe wake. As with static pressure coefficient, this raises the concern that steady flow probe calibrations against yaw angle may be invalid under unsteady flow conditions.

6. CONCLUSIONS

A series of experiments with actual sized wedge probes has been completed to more fully quantify the near wall characteristics of these instruments. From a factorial experiment in which the effect of seven variables was investigated, it was found that increasing the length of the interface piece between the probe head and stem gave a significant reduction in near wall static pressure measurement errors. Three further variables of significance were wedge head included angle, Mach number and pitch angle, where an increase in any one resulted in an accentuated static pressure wall proximity effect. Significantly different calibrations of the same probe were obtained between a closed tunnel and open jet facilities, where static pressure coefficient and yaw angle sensitivity were most altered.

Insight into the physical cause of these effects was gained from flow visualisation experiments around large scale models. Two distinct regions of re-circulating flow were identified in the probe wake, and a link between these and the flow over the wedge faces has been demonstrated. It is shown that any alteration to the re-circulations, by operating the probe near to the wall or in a free jet, will alter the static pressure and yaw angle measurement characteristics of a wedge probe. Probe calibrations obtained in steady flow may not be valid under unsteady flow conditions for similar reasons.

Acknowledgements

The authors wish to thank Rolls-Royce plc for financially supporting the work described. The views expressed are those of the authors and are not necessarily shared by the company

7. REFERENCES

Bubeck, H. and Wachter, Y., 1987, "Development and Application of a High Frequency Wedge Probe," ASME Paper 87-GT-216.

Cook, S.C.P.,1988,"Measurement Techniques for Unsteady Turbomachinery Flows," Phd Thesis, Cranfield University, Bedford.

Davies, O.L., 1978, "*The Design and Analysis of Industrial Experiments*," Second Edition, Longman Group Ltd., London.

Ferguson, T.B. and Al-Shamma, K.A., 1967, "Wedge Type Pitot-Static Probes," *BHRA SP919*, 9th Members Conference, British Hydromechanics Research Association, .Cranfield.

Fransson, T., 1983, "Aerodynamic Probe Calibrations - Results from the Workshop on Probe Calibrations, 1981 - 1983," *Proc. of 7th Symp. on Measuring Techniques for Transonic and Supersonic Flows in Cascades and Turbomachines*, Aachen.

Howard, M. et al., 1993, "Endwall Effects at Two Tip Clearances in a Multi-Stage Axial Flow Compressor with Controlled Diffusion Blading," ASME Paper 93-GT-299.

Humm, H.J. et al., 1994, "On Fast-Response Probes: Part 2 - Aerodynamic Probe Design Studies," ASME Paper 94-GT-27.

Morris, R.E., 1961, "Multiple Head Instrument for Aerodynamic Measurements," The Engineer.

Mueller, T.J., 1983, "Smoke Visualisation in Wind Tunnels," Astronautics and Aeronautics, January edition.

Shreeve, R.P.,1976, "Calibration and Application of Multiple Sensor Pneumatic Probes for Velocity Determination, with Corrections for Boundary Effects," AIAA 76-373.

Smout, P.D., 1990, "The Problem of Static Pressure Measurement in Turbomachinery Annuli Using Traversable Instrumentation," *Proc. 10th Symp. Measuring Techniques for Transonic and Supersonic Flow in Cascades and Turbomachines*, VKI, Brussels.

Smout, P.D. and Ivey, P.C., 1994, "Wall Proximity Effects in Pneumatic Measurement of Turbomachinery Flows," ASME Paper 94-GT-116.

Smout, P.D. and Ivey, P.C., 1996, "Investigation of Wedge Probe Wall Proximity Effects - Part 2: Numerical and Analytical Modelling," ASME Paper to be published.